nature cell biology

Individual dimers of the mitotic kinesin motor Eg5 step processively and support substantial loads *in vitro*

Megan T. Valentine[1,5], Polly M. Fordyce[2,5], Troy C. Krzysiak[4], Susan P. Gilbert[4] and Steven M. Block[1,3,6]

Eg5, a member of the kinesin superfamily of microtubule-based motors, is essential for bipolar spindle assembly and maintenance during mitosis, yet little is known about the mechanisms by which it accomplishes these tasks. Here, we used an automated optical trapping apparatus in conjunction with a novel motility assay that employed chemically modified surfaces to probe the mechanochemistry of Eg5. Individual dimers, formed by a recombinant human construct Eg5–513–5His, stepped processively along microtubules in 8-nm increments, with short run lengths averaging approximately eight steps. By varying the applied load (with a force clamp) and the ATP concentration, we found that the velocity of Eg5 was slower and less sensitive to external load than that of conventional kinesin, possibly reflecting the distinct demands of spindle assembly as compared with vesicle transport. The Eg5–513–5His velocity data were described by a minimal, three-state model where a force-dependent transition follows nucleotide binding.

Eg5, a Kinesin-5 (formerly known as BimC) family member, has an unusual homotetrameric protein structure that is formed by the anti-parallel arrangement of heavy chains, with pairs of heads situated at opposite ends of a common stalk[1]. In dividing cells, Eg5 is essential for the organization and maintenance of mitotic and meiotic spindles. Organized bipolar spindles contain microtubule arrays emanating from each of two focused poles, with interdigitated, anti-parallel microtubules occupying the midzone. Immunodepletion of Eg5 leads to monoastral spindles with disorganized poles and to the disruption of preformed bipolar spindles[2], and several small-molecule inhibitors of Eg5 have been identified[3,4].

However, some clues about the function of Eg5 in spindle organization are emerging. Microtubule gliding-filament assays have shown that this motor is plus-end-directed and slow, with reported velocities ranging from 10–40 nm s^{-1}(refs 2, 5–7). These velocities are similar to those of poleward flux within the spindle[4,6], suggesting that Eg5 may be involved in sliding anti-parallel microtubules relative to one another. Consistent with this, phosphorylated Eg5 motors localized to the spindle midzone[8] and pharmacological inhibition of Eg5 reduced rates of poleward flux in a dose-dependent manner[4]. Studies have also confirmed that Eg5 crosslinks anti-parallel microtubules within the midzone[8] and simultaneously moves towards the plus-ends of the two microtubules it bridges[7].

Despite recent advances, fundamental questions persist, particularly with regard to Eg5 processivity (the average number of sucessive enzymatic cycles carried out while bound to the microtubule substrate). Conventional kinesin is processive and single motors can transport cargo over large distances. In contrast, Eg5 is thought to work in small ensembles and need not be processive. A previous study used solution biochemical measurements to estimate the number of ATPase cycles per diffusion-limited encounter with the microtubule (known as 'chemical processivity') and reported that *Xenopus laevis* Eg5–437–GST dimers were less chemically processive[10] than either kinesin monomers (K340) or *Drosophila melanogaster* ncd (non-claret disjunctional, a Kinesin-14A family member) dimers (GSTMC5)[11]. Given that single-molecule experiments have directly measured the number of steps taken by single motors while bound to the microtuble (known as 'mechanical processivity') and shown that both kinesin monomers[12] and ncd[13] are mechanically nonprocessive, these chemical processivity data have been widely interpreted as evidence of nonprocessivity for Eg5 (refs 4, 7, 14). Furthermore, Eg5 motor velocity was found to depend nonlinearly on inhibitor drug concentration — an apparently cooperative phenomenon reminiscent of the nonlinear relationship between velocity and motor concentration observed in gliding-filament assays for heavy meromyosin (a soluble proteolytic fragment of muscle myosin), which is nonprocessive[4,15]. Nevertheless, uncertainty remains: a recent study[7] showed that dilute (yet multimotor) concentrations of Eg5 proteins can slide anti-parallel microtubules past one another *in vitro*, suggesting that Eg5 may be able to maintain sustained contact with microtubules. Mechanical measurements of individual Eg5 motors are required to resolve the question of processivity.

Until now, single-molecule studies of unconventional kinesins have proved challenging. First, sufficient quantities of functional, soluble motors must be obtained for analysis. Native kinesin may be purified directly from neural tissue[16], but other superfamily members generally

[1]Departments of Biological Sciences, [2]Physics, and [3]Applied Physics, Stanford University, Stanford, CA 94305, USA. [4]Department of Biological Sciences, University of Pittsburgh, Pittsburgh, PA 15260, USA. [5]These authors contributed equally to this work.
[6]Correspondence should be addressed to S.M.B. (e-mail: sblock@stanford.edu)

Received 10 January 2006; accepted 15 March 2006; published online 2 April 2006; DOI: 10.1038/ncb1394

©2006 Nature Publishing Group

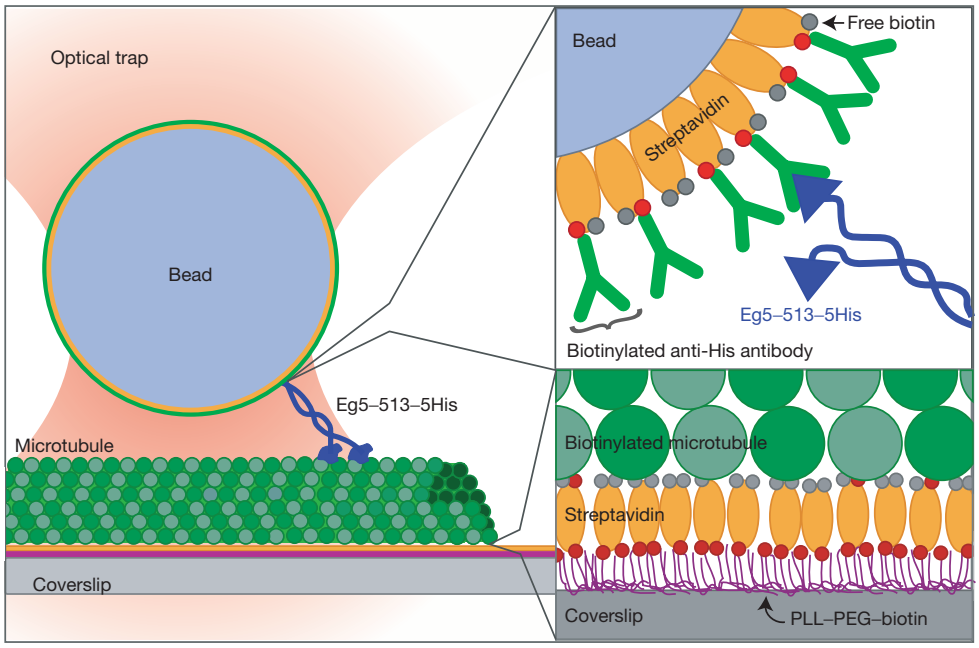

Figure 1 Schematic representation of the experimental geometry (not to scale). A His-tagged Eg5 homodimer (dark blue) is attached to a bead (light blue) maintained in an optical trap (pink) as it walks along a surface-attached microtubule (green). Details of the Eg5-bead linkage are shown on the top right. His-tagged motors were linked stereospecifically to streptavidin-coated polystyrene beads through a biotinylated anti-pentaHis antibody. The remaining binding sites were quenched by the addition of excess biotin. Details of the microtubule-surface linkage are shown on the bottom right. The coverglass surface was treated with biotinylated poly(L-lysine)–graft–polyethylene glycol block copolymers (PLL–PEG–biotin) to prevent non-specific adsorption of Eg5. Positively charged PLL blocks self-assemble through non-specific electrostatic interactions, while the neutral PEG chains form a dense layer that extends into solution, providing a barrier against protein adsorption. Biotinylated microtubules were specifically bound to this copolymer surface through streptavidin linkages.

require the development of a recombinant expression system. Second, an *in vitro* motility assay must be established for the purified motor that functions robustly for single molecules. Third, the motor must generate processive motion if some of the more informative mechanochemical properties are to be measured (such as stall force, step size or motor velocity as a function of load or ATP concentration).

For Eg5, the first of these challenges was met by developing a recombinant system to express the initial 513 amino (N)-terminal amino acids of the cloned human heavy chain followed by a carboxy (C)-terminal pentahistidine tag (Eg5–513–5His). This construct encodes the catalytic core and extends to the first predicted break in the coiled-coil stalk, and forms stable, soluble dimers after purification when expressed in *Escherichia coli* (see Supplementary Information, Fig. S1). In multiple motor microtubule-gliding assays, Eg5–513–5His dimers produced movement at speeds comparable to full-length Eg5 tetramers[2,7].

Traditional single-molecule, bead-based motility assays rely on fortuitous surface interactions peculiar to microtubules and conventional kinesin[9]. Under appropriate buffer conditions, microtubules bind non-specifically to charged coverglass surfaces, but kinesin-coated beads do not. However, this assay must be significantly adapted for use with other kinesin-related motors. Eg5-coated polystyrene beads adhered to coverglasses over a wide range of experimental conditions, even in the presence of blocking proteins (for example, casein or bovine serum albumin). To overcome this problem, an assay using chemically modified coverglass surfaces with functionalized polyethylene glycol (PEG) chains that repel motor-coated beads, while achieving specific attachment of microtubules, was developed (Fig. 1).

When placed by the optical trap near surface-attached microtubules, Eg5–513–5His-coated beads bound, and subsequently moved, over a range of loading conditions and ATP levels (Fig. 2a–f). Records of bead motion obtained in the single-molecule limit displayed a series of discrete steps, with average step size (d) = 8.1 ± 0.1 nm, consistent with the spacing of tubulin heterodimers along a protofilament (see Supplementary Information, Fig. S2), and identical to the step size of conventional kinesin[17]. To determine the minimal number of dimeric motors required to move a bead, individual beads were captured, positioned against a microtubule and the fraction that bound and moved was scored as a function of the dimer concentration, C (Fig. 2g). This distribution was well fit by the Poisson probability that the bead carried one or more motors ($\chi^2_\nu = 0.5$; number of degrees of freedom (ν) = 5; $P(\chi^2_\nu) = 0.78$), demonstrating that a single Eg5 dimer is sufficient to transport a bead[18]. Processive run lengths were measured in the absence of load for individual records. An exponential fit to the corresponding histogram yielded a mean distance of 67 ± 7 nm (Fig. 2h). Based on the measured step size of 8.1 nm, the mechanical processivity for Eg5–513–5His is 8.3 steps per run, in contrast with kinesin, whose unloaded processivity is approximately 100 steps per run[9]. Additional force-clamped measurements showed that the run length did not depend strongly on the applied force or ATP concentration (see Supplementary Information, Fig. S3).

To probe rates of nucleotide binding and catalysis, Eg5–513–5His velocity was measured as a function of ATP concentration at different fixed loads (Fig. 3a). Velocities for single Eg5 dimers were consistently two- to threefold faster than those of Eg5 tetramers measured under multiple-motor conditions in gliding-filament or spindle-assembly assays[2,5–7]. This difference may arise from negatively cooperative effects

©2006 Nature Publishing Group

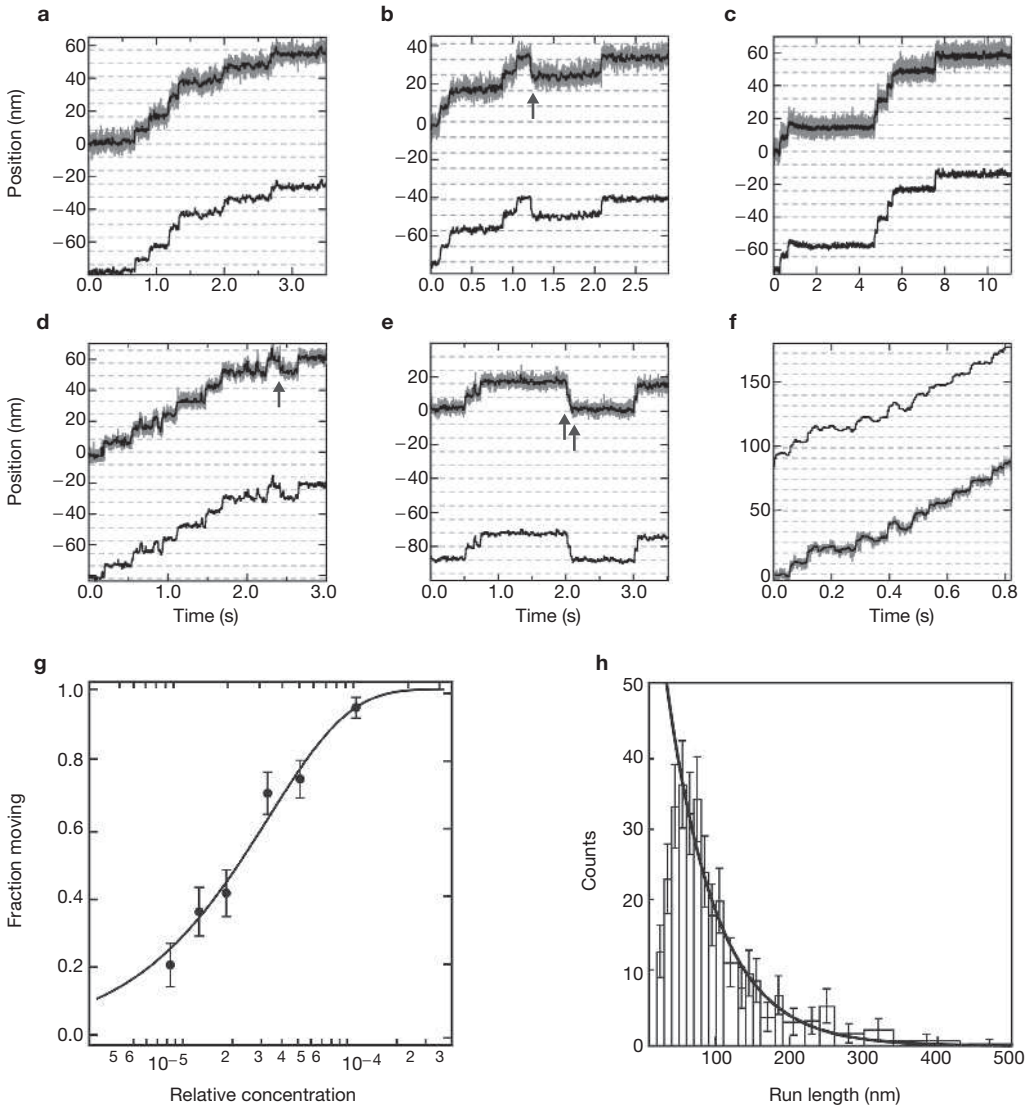

Figure 2 Single Eg5–513–5His dimers are processive. (**a**–**f**) Representative records of bead motion in the force clamp driven by single Eg5–513–5His dimers showing 8-nm steps. Occasional back-steps are also observed at high loads (grey arrows). Median-filtered bead position (25-point window, black trace) is superimposed on the unfiltered position (grey trace). Trap position (black trace) is offset from bead position by computer feedback, supplying constant load. Experimental conditions: load = –4 pN and ATP concentration = 8 μM in **a**, **b** and **d**; load = –4 pN and ATP concentration = 2 mM in **c**; load = –4 pN and ATP concentration = 31 μM in **e**; load = +4 pN and ATP concentration = 2 mM in **f**. (**g**) Fraction of Eg5–513–5His-coated beads moving as a function of the relative motor concentration. If a single dimer suffices to transport a bead, then the fraction of moving beads, ρ, corresponds to the Poisson probability that the bead carries one or more dimers, given by $\rho(C) = 1-\exp(-\lambda C)$, where λ is a single parameter[18]. The data fit this function ($\chi^2_\nu = 0.5$; $\nu = 5$; $P(\chi^2_\nu) = 0.78$). Values are expressed as $\rho \pm [\rho(1-\rho)/n]^{1/2}$ ($N = 323$ total measurements; $n = 43$–66 at each concentration). If two or more dimers were required, then $\rho(C) = 1-\exp(-\lambda C)-\lambda C\exp(-\lambda C)$. This fit was significantly poorer ($\chi^2_\nu = 2.0$; $\nu = 5$; $P(\chi^2_\nu) = 0.075$). (**h**) Histogram of run lengths for Eg5–513–5His dimers at zero load ($N = 1{,}592$). Fit to a single exponential (excluding first 3 bins) returned a mean run length of 67 ± 7 nm ($\chi^2_\nu = 0.57$; $\nu = 12$; $P(\chi^2_\nu) = 0.84$, 2 parameters).

among multiple motors in earlier work, but it is more likely to follow from improvements in surface chemistry that suppress nonspecific binding in this assay. Fits of these data to the Michaelis-Menten relation supplied a maximum velocity (v_{max}) of 96 ± 2 nm s^{-1} in the absence of load and 56 ± 2 nm s^{-1} under –4 pN of load (where negative values indicate loads opposing motor motion[19]). The apparent Michaelis constant (K_M, the ATP concentration producing half-maximal velocity) can be combined with the turnover rate (k_{cat}, the stepping rate at saturating ATP, where $k_{cat} = v_{max}/d$) to calculate the apparent second-order rate constant for ATP binding ($k_b = k_{cat}/K_M$). For both Eg5 and conventional kinesin, strong hindering loads reduce both k_{cat} and k_b, constraining potential kinetic models by requiring that any force-dependent transition occurs after nucleotide binding but no later than the first irreversible transition. In contrast with conventional kinesin (where K_M increases with increasing load[9]) the K_M for Eg5 was load-independent (14 ± 1 μM for both 0 pN and –4 pN loads; Table 1), possibly reflecting differences in nucleotide affinity between the two motors (see Supplementary Information). The K_M measurements agree with values determined from steady-state solution kinetics for Eg5–513 (8 ± 2 μM) and for Eg5–513–5His (10 ± 2 μM; data not shown). However, the value for k_{cat} determined from single-molecule velocities at zero force (11.9 ± 0.2 s^{-1}) was significantly higher than that measured by steady-state solution kinetics for either

©2006 Nature Publishing Group

Table 1 Kinetic parameters of Eg5–513–5His

Constants		Values and errors
Steady-state turnover rate ($F = 0$)	k_{cat}	11.9 ± 0.2 s^{-1}
Michaelis constant	K_M	15 ± 2 μM
ATP binding	k_1	0.89 ± 0.07 $\mu M^{-1} s^{-1}$
ATP unbinding	k_{-1}	10 ± 4 s^{-1}
Force-dependent translocation	k_2^0	86 ± 21 s^{-1}
Distance to transition state	δ_2	1.9 ± 0.2 nm
Irreversible biochemical transition	k_3	13.5 ± 0.5 s^{-1}

Eg5–513 (0.48 ± 0.02 s^{-1}) or Eg5–513–5His (0.45 ± 0.04 s^{-1}; data not shown). The limited processivity of Eg5 may cause solution studies to underestimate the value of k_{cat}, as frequent detachments from microtubules reduce the concentration of active motors that contribute to the overall reaction rate.

The application of force selectively affects rate constants associated with mechanical transitions[20]. To examine the effects of force on Eg5 kinetics, velocity was measured as a function of applied load at fixed ATP concentrations (Fig. 3b). For assisting loads between 0 and 4 pN, no significant effect of force on velocity for saturating ATP concentrations or when ATP concentrations were approximately equal to K_M was observed. Hindering loads reduced velocities to half-maximal at approximately –4 pN in both cases.

The simplest kinetic model that can explain these velocity data is a three-state model with a single force-dependent transition shared between k_b and k_{cat} (Fig. 3c). In this minimal scheme, reversible ATP binding is followed by a load-dependent translocation plus an irreversible step representing a composite biochemical transition, including events such as ATP hydrolysis or product release. Global model fits are plotted in Fig. 3a and b and the parameters are summarized in Table 1. The ATP binding and unbinding rate constants for dimeric Eg5 (k_1 and k_{-1}, respectively) are in close agreement with those determined by presteady-state solution kinetics (data not shown). The load-dependent transition rate (k_2) is rapid and at saturating ATP concentrations and zero force, the biochemical transition (k_3) is rate limiting at 13 s^{-1}. The apparent distance to the transition state (δ_2) is smaller for Eg5 than for conventional kinesin (1.9 nm versus 2.7 nm[19]), suggesting a mechanistically different load-dependent transition. Consistent with this, crystal structures have revealed that in the ADP-bound state, the kinesin neck linker (thought to be critical for controlling directionality[21] and maintaining processivity[22]) is disordered and flexible, whereas for Eg5 it is well-ordered and aligned perpendicular to the microtubule axis[14,23,24]. Our results indicate that the apparently rigid neck linker of Eg5 does not abolish processivity, but this inflexibility may introduce subtle differences in the production of force.

In contrast with conventional kinesin, which slows and stalls under high hindering loads[19], Eg5 motors tended to dissociate from microtubules before slowing substantially. As measurements of velocity require some persistence of motion, the highest force at which velocity was determined (–5 pN) does not faithfully represent the greatest load that Eg5 motors can sustain. An improved estimate (lower bound) of the Eg5 stall force was obtained by recording the progress of motors stepping processively out of a fixed optical trap at high stiffness (see Supplementary Information, Fig. S4). In this experiment, some Eg5 dimers sustained loads as high as –7 pN, although most motors dissociated at lower forces.

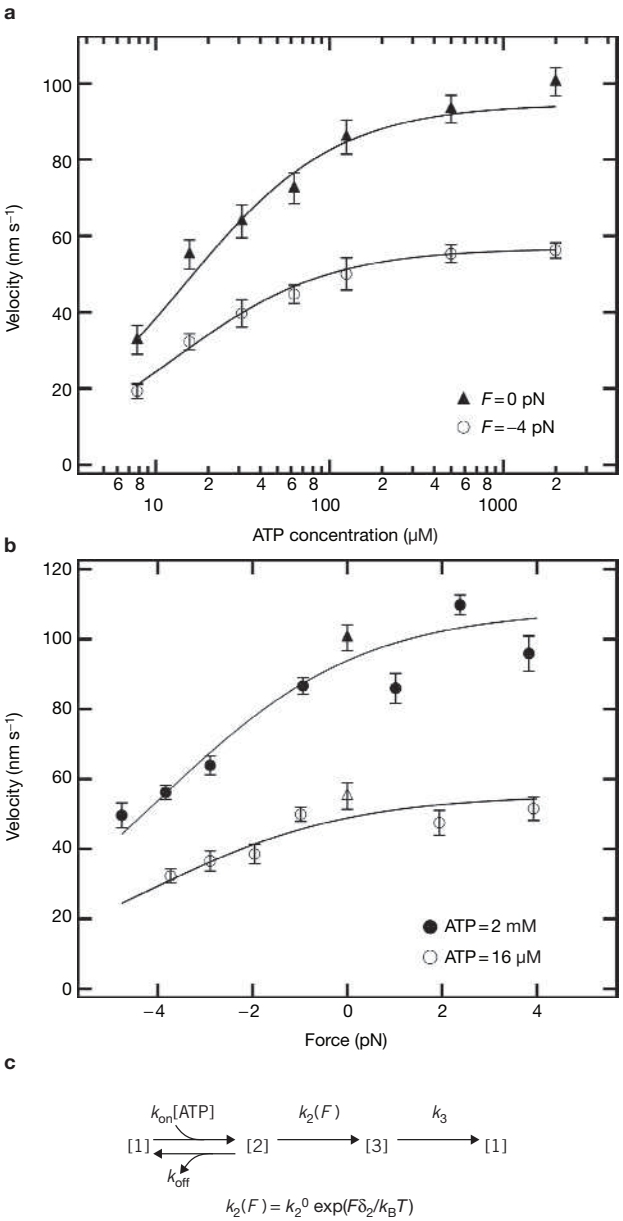

Figure 3 Eg5 velocity as a function of ATP concentration and force with global model fits. Negative forces denote hindering loads. Both force-clamped data (circles) and unloaded video-tracked data (triangles) are plotted. (**a**) Velocity (weighted mean ± s.e.m.) versus ATP concentration at $F = 0$ pN (solid triangles; $n = 22$–67) and $F = -4$ pN (open circles; $n = 29$–92). (**b**) Velocity (weighted mean ± s.e.m.) versus applied force at ATP concentration = 2 mM (solid points; $n = 70$–212) and ATP concentration = 16 μM (open points; $n = 57$–80). (**c**) Reaction pathway for a minimal, three-state model of the Eg5 mechanochemical cycle. Reversible nucleotide binding is followed by an irreversible load-dependent translocation step and an irreversible biochemical transition with no associated displacement. An alternative model explicitly incorporating a reversible, load-dependent transition returned a best-fit rate of zero for the back reaction (k_{-2}). Therefore, this step was taken to be irreversible. Rate constants and transition state distances derived from a global fit of this model to the data are shown in Table 1.

To determine the number of ATP molecules consumed per 8-nm step, a fluctuation analysis of motion as a function of ATP concentration and load[25], was performed. The randomness parameter, r, provides a measure of the stochasticity of enzyme movements[25–27]. A value of $r = 0$ indicates

©2006 Nature Publishing Group

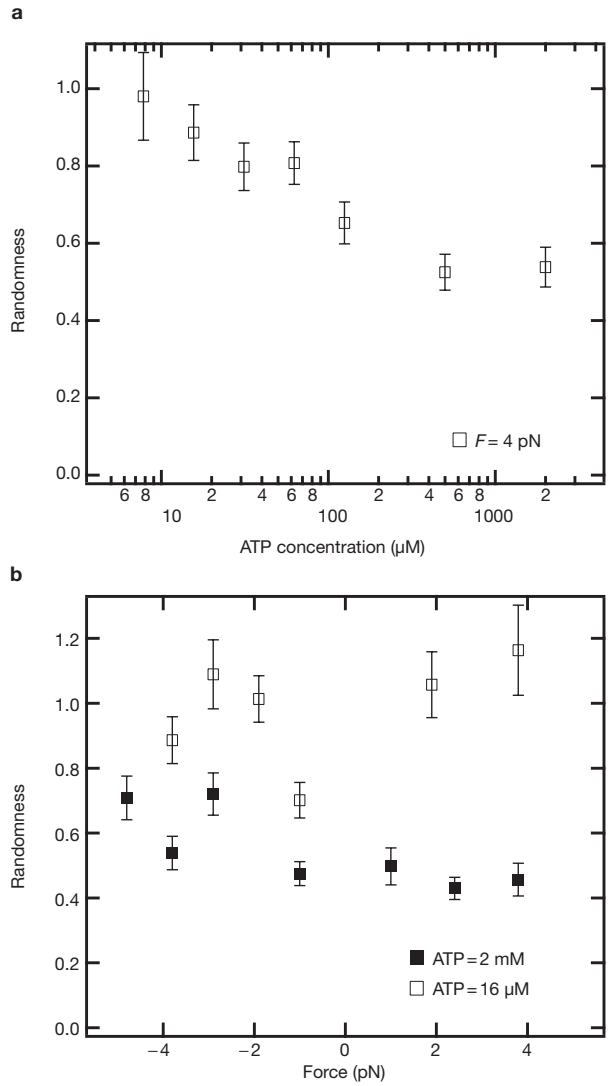

Figure 4 Eg5 randomness as a function of ATP and force. (**a**) Randomness (weighted mean ± s.e.m.) versus ATP concentration for $F = -4$ pN (open squares; $n = 27–86$). In saturating ATP conditions (2 mM), where nucleotide binding is rapid and therefore cannot be rate-limiting, the value of r asymptotes to appromimately 0.5, indicative of at least two rate-limiting transitions in the reaction cycle, in addition to nucleotide binding. For limiting ATP concentrations, randomness increases towards unity, implying that one ATP molecule is hydrolysed per step. (**b**) Randomness (weighted mean ± s.e.m.) versus force for ATP concentration = 2 mM (solid squares; $n = 62–212$) and ATP concentration = 16 μM (open squares; $n = 53–73$). At limiting ATP concentrations, randomness is near unity for nearly all applied loads, reflecting that ATP binding remains the solitary, rate-limiting transition. At saturating ATP concentrations and high hindering loads, r increases as the completion time of the force-dependent transition begins to dominate the reaction cycle. For saturating ATP concentrations and high assisting loads, where neither nucleotide binding nor translocation are rate-limiting, r asymptotes to approximately 0.4, indicative of the presence of at least two additional steps in the reaction cycle.

a perfectly regular (clock-like) process, whereas $r = 1$ corresponds to a Poisson process with exponentially distributed waiting times. For biochemical pathways consisting of a linear sequence of events, r^{-1} supplies a measure of the number of rate-limiting transitions. r was first calculated for stepping records obtained at –4 pN load over a range of ATP concentrations. For reduced ATP concentrations, r increased towards unity as ATP binding became the solitary rate-limiting transition, establishing that a single ATP molecule was hydrolysed per step, as previously observed for conventional kinesin[25] (Fig. 4a).

To further explore the load-dependent transitions of Eg5–513–5His, the relationship between randomness and force was determined under two different ATP concentrations (Fig. 4b). For saturating ATP concentrations and assisting loads, r approached a value of 0.4, indicative of at least two additional transitions besides ATP binding and motor translocation, both of which are rapid under these conditions. Therefore, fluctuation analysis implies the existence of at least four potentially rate-limiting transitions within the mechanochemical reaction cycle of Eg5. Fluorescence resonance energy transfer (FRET) studies have suggested that Eg5, unlike kinesin, may move in two distinct motions — an ATP-dependent docking of the neck linker followed by a rotation of the head on the microtubule[28]. Consistent with this observation, kinetic models including more than five transitions are required to capture the qualitative features of the randomness data (fit not shown). However, solutions to such complex models based on currently available data are degenerate and preclude a unique determination of rate constants.

Our results show that Eg5 dimers undertake multiple steps along microtubules before dissociating, although run lengths were modest, averaging approximately eight steps. Eg5 motors remained processive even when subjected to strong loads, signifying that at least one motor head remains bound to the microtubule throughout the mechanochemical cycle. These findings suggest that chemical processivity, estimated biochemically, is a poor predictor of mechanical behaviour for weakly processive motors. Furthermore, the nonlinear (and apparently cooperative) dose-dependence reported for the pharmacological inhibition of poleward spindle flux, previously interpreted as evidence of nonprocessivity[4], may require an alternative explanation. Pharmacologically inhibited Eg5 motors may remain weakly bound to microtubules, thereby reducing the ability of the remaining motors to slide the very same microtubules[29] and producing an apparently cooperative dose-response. Eg5 processivity may also necessitate revisions to models of mitosis that rely on Eg5 tetramers making only transient interactions with spindle microtubules, or that invoke a non-microtubule 'spindle matrix' to explain why motors remain anchored at specific cellular locations[5].

The processivity of Eg5 allows an unprecedented comparison of the mechanochemistry of two kinesin superfamily members. In many ways, Eg5 dimers and conventional kinesin are similar: both are plus-end-directed motors that take 8-nm steps along microtubules; they both hydrolyse one ATP per advance; and they both obey Michaelis-Menten kinetics. Neither motor accelerates strongly under assisting loads, and both slow monotonically under hindering loads (with reduced rates for both k_{cat} and k_b), supporting forces up to approximately 7 pN. When advancing towards stall, both Eg5 and kinesin dissipate approximately 60 pN nm of energy per step (8.1 nm × ~7 pN), representing two-thirds or more of the free energy available from ATP hydrolysis[30]. There are, however, salient differences. Eg5 is dramatically slower, moving at unloaded speeds of only 100 nm s^{-1} at saturating ATP concentrations, whereas kinesin moves 6- to 8-fold faster under similar conditions[31]. Although processive, Eg5 averages fewer than 10 steps per run, whereas kinesin takes 100 steps or more[9,20]. Eg5 and kinesin also differ substantially in their responses to hindering loads. Our minimal model returns a transition state distance for Eg5 that is slightly smaller than that of kinesin and the overall effect of load on Eg5 kinetics is less dramatic. At saturating ATP concentrations, the application of –5 pN load reduces

©2006 Nature Publishing Group

the overall catalytic rate for Eg5 by approximately twofold, whereas the equivalent rate for kinesin is slowed by approximately 15-fold[19]. At high hindering loads, kinesin velocity slows to near zero and stalls, whereas Eg5 tends to dissociate.

We speculate that the distinct behaviours of kinesin and Eg5 under load may reflect differences in their physiological roles. *In vivo*, increases in load for kinesin may signal that its cargo has encountered an obstacle. In this case, the motor slows, thus avoiding futile ATP hydrolysis[20] and promoting detachment. In contrast, Eg5 must continue sliding microtubules during spindle elongation even while maintaining substantial tension, leading to relatively load-insensitive turnover rates. Furthermore, the tendency of single Eg5 motors to detach, rather than stall, at high loads may prevent individually stuck motors from interfering with ensemble-driven sliding.

It is not obvious why processivity is important for a motor that works mainly in ensembles. If the pairs of heads located at either end of the native homotetramer move independently, then the probability of detachment for the tetramer will be the product of the probabilities of detachment for each pair of heads, yielding a predicted run length of 64 steps (approximately 0.5 μm). This limited processivity may permit individual Eg5 motors to localize rapidly to the midzone during the onset of mitosis, forming a critical ensemble. Moreover, processivity may be important for maintaining mechanical integrity early in spindle assembly, when few microtubules or motors may be present. Later during assembly, efficient spindle maintenance may require that many Eg5 motors work together in groups. It seems possible that Eg5 motors have evolved to satisfy competing demands. □

METHODS

Cloning and protein expression. Eg5–513–5His was engineered using the coding sequence for the N-terminal 513 residues (Met 1–Leu 513) of the human *Eg5* gene. This region was PCR-amplified from a pBluescript plasmid containing the full-length human *Eg5* cDNA (generous gift from A. Blangy, Centre de Recherches de Biochimie Macromoléculaire, Montpellier, France). Amplification used 5′-GCGTATGGCCAAACTGGCAC as the N-terminal primer, and 5′-ATCCAGCTCGAGTTAGTGGTGGTGGTGGTGCATGGCCTTGTGGAGACCAGATACATC as the C-terminal primer. The C-terminal primer inserted a short peptide linker and a pentahistidine tag before the stop codon and *Xho*1 restriction site. A pRSETa plasmid containing the Eg5–513–5His sequence was then transformed into the BL21–CodonPlus(DE3)–RIL cell line (Stratagene, La Jolla, CA) for protein expression (predicted molecular weight (M_r) = 58,797 per monomer). The expressed protein was purified by microtubule affinity and its dimeric state was confirmed by analytical gel filtration (see Supplementary Information, Fig. S1).

Assays. Biotinylated microtubules were prepared by polymerizing a 1:10 mixture of biotinylated and unmodified purified bovine brain tubulin (Cytoskeleton, Denver, CO) at a final concentration of 1.9 mg ml^{-1} in polymerization buffer (62 mM PIPES at pH 6.9, 0.8 mM EGTA, 3.7 mM $MgCl_2$, 0.9 mM GTP and 10% v/v DMSO) for 1 h at 37 °C. Microtubules were stabilized by the addition of 5 μM taxol. To remove free tubulin, microtubules were layered over a 15% w/v sucrose cushion in stablilzation buffer (80 mM PIPES at pH 6.9, 1.7 mM EGTA, 5.5 mM $MgCl_2$, 1.2 mM GTP, 8.2 mM sodium azide, 20 μM taxol and 10% v/v DMSO) and centrifuged at 26,000*g* for 15 min at 30 °C. The pellet was resuspended in stabilization buffer. Steady-state ATPase measurements showed that Eg5–513–5His kinetics were unaffected by the biotinylation of microtubules (data not shown).

To prepare beads for coupling to tagged Eg5 proteins, 0.44 μm-diameter streptavidin-coated polystyrene beads (Spherotech, Libertyville, IL) were incubated with biotin-conjugated anti-pentaHis antibodies (Qiagen, Valencia, CA) for 1 h followed by washing and resuspension in 100 mM phosphate buffer at pH 7.5 with 0.1% Tween-20. Beads were then incubated with Eg5–513–5His in assay buffer based on PEM80 (80 mM PIPES at pH 6.9, 1 mM EGTA and 4 mM $MgCl_2$) with 200 mM KCl, 50 mM potassium acetate, 2 mM DTT, 7 μM taxol, 200 nM ATP and excess free biotin at 4 °C for 3–9 h. Longer incubation times resulted in decreased motor activity. Eg5 concentrations used were sufficiently dilute that fewer than one motor, on average, bound to each bead. Consistent with previous studies, addition of 200 mM KCl was necessary to obtain consistent Eg5 motion[1,2]. An oxygen-scavenging system (250 μg ml^{-1} glucose oxidase, 30 μg ml^{-1} catalase and 4.5 μg ml^{-1} glucose) and the desired concentration of ATP were added to Eg5-coated beads in assay buffer immediately before measurement.

Flow cells were assembled from glass slides and plasma-cleaned coverglasses. To reduce nonspecific binding of Eg5-coated beads to the coverglass, the surface was incubated with biotinylated poly-L-lysine–graft–polyethylene glycol copolymers (SurfaceSolutionS, Zurich, Switzerland) for 30 min. Excess copolymer was washed away and the surface was incubated with 0.2 mg ml^{-1} SA20 streptavidin (Prozyme, San Leandro, CA) for 10 min. Excess streptavidin was washed out and biotinylated microtubules (diluted in PEM80 with 10 μM taxol) were introduced and incubated for 15 min or longer to allow specific attachment to the surface through the streptavidin linkage. Free microtubules were washed out with assay buffer and the Eg5-coupled beads were introduced into the sample chamber.

Instrumentation. The optical trapping instrument used in this experiment has been previously described[32]. Briefly, a computer-controlled, steerable optical trap was used to apply either variable or constant loads (in a force clamp arrangement) to individual bead-attached motors. Bead motion was measured through light scattering from a separate, single-mode diode laser onto a position sensitive detector (PSD, Pacific Silicon Sensors, Westlake Village, CA). For video-tracking of unloaded beads, differential interference-contrast images were acquired with a video capture card (National Instruments, Austin, TX), and bead position was determined using a centroid tracking algorithm on individual frames with sub-pixel accuracy.

Calibration and data collection. For video-tracking, weakly trapped Eg5-coated beads were placed near a microtubule and bead position was monitored. When the data-acquisition software detected that the bead had moved approximately 35 nm from the trap centre, the computer shuttered the trap and recorded the bead position at video rates for the duration of the run. Beads were recaptured after detachment and returned to their starting position. For all velocity measurements under load, an automated force clamp[19] was used to apply longitudinal assisting or hindering loads of 1–6 pN in magnitude to Eg5-coated beads. Automated positioning and calibration procedures performed before each bead measurement enhanced the reproducibility and reduced measurement error. First, the piezoelectric stage was used to position a captured bead 150 ± 25 nm above the coverglass surface. To avoid calibration errors resulting from small variations in bead diameters, the PSD response for each bead was determined separately by raster scanning the bead over the detection region[33]. Trap stiffness was determined by measuring both the mean squared displacement and the corner frequency of the Lorentzian power spectrum for a trapped bead[34]; only records where these two estimates of stiffness agreed within 20% were used. Bead and trap positions in both *x*- and *y*-dimensions were sampled at 2 kHz and Bessel-filtered at 1 kHz. Trap stiffnesses ranged from 0.01–0.06 pN nm^{-1}. In force clamp mode, trap position trailed bead position by an offset of 70–90 nm. Maximal (stall) force measurements (N = 85) were made using a fixed-position optical trap at high stiffness (approximately 0.09–0.12 pN nm^{-1}).

Data analysis. For measurements of the fraction of beads moving as a function of the relative motor concentration, each bead was tested on at least three different microtubules before scoring. To account for small decreases in motor activity over time, each sample dilution was measured twice at different times.

Average velocity, v, was determined by dividing distance travelled by the time taken for each run and weighting this measurement by the run length. To determine the randomness for each run, the variance was calculated, $\{x(t + \Delta t) - (x(t) + \langle v \rangle \Delta t)\}^2$, as a function of Δt, where the brackets indicate an average over all runs at that condition. A linefit was performed to this variance over the first 20 nm $\langle v \rangle^{-1}$ time interval, excluding the first 3.5 ms to account for the bead viscous relaxation time[25]. Randomness, r, was calculated from the slope of the variance versus Δt, divided by $d\langle v \rangle$. Average randomness values were

©2006 Nature Publishing Group

weighted by run length. Errors were calculated by averaging the standard deviations weighted by run length and dividing by the number of events (standard error). Average run lengths were calculated by fitting a histogram of individual run lengths to a single exponential with the offset fixed at zero. Minimum bin width was 10 nm and each bin contained at least six points. Global fits of all velocity data were performed, as a function of both force and ATP concentration, to a three-state model to derive the kinetic parameters (Fig. 3c). Velocities, v, were fit to $v = dk_1[\mathrm{ATP}]k_2k_3/\{k_1[\mathrm{ATP}](k_2 + k_3) + k_3(k_2 + k_{-1})\}$, where k_1 is the second-order rate constant for nucleotide binding, k_{-1} is the rate of nucleotide unbinding and k_3 is the rate of a final irreversible transition. The force-dependent rate k_2 incorporates an Arrhenius-Boltzmann factor, $k_2 = k_2^0 \exp(F\delta_2/k_BT)$, where k_2^0 is the unloaded rate constant, δ_2 is the distance to the transition state along the reaction coordinate, F is the applied load and k_BT is the thermal energy.

Note: Supplementary Information is available on the Nature Cell Biology website.

ACKNOWLEDGEMENTS

This work was supported by grants to S.M.B. and S.P.G. from the National Institutes of Health (NIH). M.T.V. was supported by a Career Award at the Scientific Interface from the Burroughs Wellcome Fund. P.M.F. was supported by a predoctoral fellowship from the National Science Foundation (NSF) and a Lieberman fellowship. We thank W. Greenleaf, N. Guydosh and J. Burney for careful reading of the manuscript, and J. Shaevitz, C. Asbury and Block laboratory members for helpful discussions.

AUTHOR CONTRIBUTIONS

P.M.F. and M.T.V. designed, performed and analysed the single-molecule experiments and co-wrote the manuscript. T.C.K. and S.P.G. generated the Eg5 constructs and conducted the biochemical measurements. S.M.B. and S.P.G. supplied guidance, designed research and edited the manuscript.

COMPETING FINANCIAL INTERESTS

The authors declare that they have no competing financial interests.

Published online at http://www.nature.com/naturecellbiology/
Reprints and permissions information is available online at http://npg.nature.com/reprintsandpermissions/

1. Kashina, A., Rogers, G. & Scholey, J. M. The bimC family of kinesins: essential bipolar mitotic motors driving centrosome separation. *Biochim. Biophys. Acta.* **1357,** 257–271 (1997).
2. Sawin, K. E., LeGuellec, K., Philippe, M. & Mitchison, T. J. Mitotic spindle organization by a plus-end-directed microtubule motor. *Nature* **359,** 540–543 (1992).
3. Mayer, T. U. *et al.* Small molecule inhibitor of mitotic spindle bipolarity identified in a phenotype-based screen. *Science* **286,** 971–974 (1999).
4. Miyamoto, D. T., Perlman, Z. E., Burbank, K. S., Groen, A. C. & Mitchison, T. J. The kinesin Eg5 drives poleward microtubule flux in *Xenopus laevis* egg extract spindles. *J. Cell Biol.* **167,** 813–818 (2004).
5. Kapoor, T. M. & Mitchison, T. J. Eg5 is static in bipolar spindles relative to tubulin: evidence for a static spindle matrix. *J. Cell Biol.* **154,** 1125–1133 (2001).
6. Kwok, B. H., Yang, J. G. & Kapoor, T. M. The rate of bipolar spindle assembly depends on the microtubule-gliding velocity of the mitotic kinesin Eg5. *Curr. Biol.* **14,** 1783–1788 (2004).
7. Kapitein, L. C. *et al.* The bipolar mitotic kinesin Eg5 moves on both microtubules that it crosslinks. *Nature* **435,** 114–118 (2005).
8. Sharp, D. J. *et al.* The bipolar kinesin, KLP61F, cross-links microtubules within interpolar microtubule bundles of *Drosophila* embryonic mitotic spindles. *J. Cell Biol.* **144,** 125–138 (1999).
9. Block, S. M., Goldstein, L. S. & Schnapp, B. J. Bead movement by single kinesin molecules studied with optical tweezers. *Nature* **348,** 348–352 (1990).
10. Hackney, D. D. Highly processive microtubule-stimulated ATP hydrolysis by dimeric kinesin head domains. *Nature* **377,** 448–450 (1995).
11. Crevel, I. M., Lockhart, A. & Cross, R. A. Kinetic evidence for low chemical processivity in ncd and Eg5. *J. Mol. Biol.* **273,** 160–170 (1997).
12. Kamei, T., Kakuta, S. & Higuchi, H. Biased binding of single molecules and continuous movement of multiple molecules of truncated single-headed kinesin. *Biophys. J.* **88,** 2068–2077 (2005).
13. deCastro, M. J., Fondecave, R. M., Clarke, L. A., Schmidt, C. F. & Stewart, R. J. Working strokes by single molecules of the kinesin-related microtubule motor ncd. *Nature Cell Biol.* **2,** 724–729 (2000).
14. Turner, J. *et al.* Crystal structure of the mitotic spindle kinesin Eg5 reveals a novel conformation of the neck-linker. *J. Biol. Chem.* **276,** 25496–25502 (2001).
15. Uyeda, T. Q., Kron, S. J. & Spudich, J. A. Myosin step size. Estimation from slow sliding movement of actin over low densities of heavy meromyosin. *J. Mol. Biol.* **214,** 699–710 (1990).
16. Vale, R. D. *et al.* Direct observation of single kinesin molecules moving along microtubules. *Nature* **380,** 451–453 (1996).
17. Svoboda, K., Schmidt, C. F., Schnapp, B. J. & Block, S. M. Direct observation of kinesin stepping by optical trapping interferometry. *Nature* **365,** 721–727 (1993).
18. Svoboda, K. & Block, S. M. Force and velocity measured for single kinesin molecules. *Cell* **77,** 773–784 (1994).
19. Block, S. M., Asbury, C. L., Shaevitz, J. W. & Lang, M. J. Probing the kinesin reaction cycle with a 2D optical force clamp. *Proc. Natl Acad. Sci. USA* **100,** 2351–2356 (2003).
20. Schnitzer, M. J., Visscher, K. & Block, S. M. Force production by single kinesin motors. *Nature Cell Biol.* **2,** 718–723 (2000).
21. Endow, S. A. & Waligora, K. W. Determinants of kinesin motor polarity. *Science* **281,** 1200–1202 (1998).
22. Thorn, K. S., Ubersax, J. A. & Vale, R. D. Engineering the processive run length of the kinesin motor. *J. Cell Biol.* **151,** 1093–1100 (2000).
23. Sindelar, C. V. *et al.* Two conformations in the human kinesin power stroke defined by X-ray crystallography and EPR spectroscopy. *Nature Struct. Mol. Biol.* **9,** 844–848 (2002).
24. Rice, S. *et al.* A structural change in the kinesin motor protein that drives motility. *Nature* **402,** 778–784 (1999).
25. Schnitzer, M. J. & Block, S. M. Kinesin hydrolyses one ATP per 8-nm step. *Nature* **388,** 386–390 (1997).
26. Schnitzer, M. J. & Block, S. M. Statistical kinetics of processive enzymes. *Cold Spring Harb. Symp. Quant. Biol.* **60,** 793–802 (1995).
27. Shaevitz, J. W., Block, S. M. & Schnitzer, M. J. Statistical kinetics of macromolecular dynamics. *Biophys. J.* **89,** 2277–2285 (2005).
28. Rosenfeld, S. S., Xing, J., Jefferson, G. M. & King, P. H. Docking and rolling — a model of how the mitotic motor Eg5 works. *J. Biol. Chem.* **280,** 35684–35695 (2005).
29. Crevel, I. M., Alonso, M. C. & Cross, R. A. Monastrol stabilises an attached low-friction mode of Eg5. *Curr. Biol.* **14,** R411–R412 (2004).
30. Block, S. M. Nanometres and piconewtons: the macromolecular mechanics of kinesin. *Trends Cell Biol.* **5,** 169–175 (1995).
31. Visscher, K., Schnitzer, M. J. & Block, S. M. Single kinesin molecules studied with a molecular force clamp. *Nature* **400,** 184–189 (1999).
32. Lang, M. J., Fordyce, P. M., Engh, A. M., Neuman, K. C. & Block, S. M. Simultaneous, coincident optical trapping and single-molecule fluorescence. *Nature Methods* **1,** 133–139 (2004).
33. Lang, M. J., Asbury, C. L., Shaevitz, J. W. & Block, S. M. An automated two-dimensional optical force clamp for single molecule studies. *Biophys. J.* **83,** 491–501 (2002).
34. Neuman, K. C. & Block, S. M. Optical trapping. *Rev. Sci. Instrum.* **75,** 2787–2809 (2004).

©2006 Nature Publishing Group

Supplementary Information for:

Individual dimers of the mitotic kinesin motor Eg5 step processively and support substantial loads *in vitro*

M. T. Valentine[1,*], Polly M. Fordyce[2,*], Troy C. Krzysiak[3], Susan P. Gilbert[3], and Steven M. Block[1,4,5]

[1]Departments of Biological Sciences, [2]Physics, and [4]Applied Physics, Stanford University, Stanford, CA 94305, USA. [3]Department of Biological Sciences, University of Pittsburgh, Pittsburgh, PA 15260, USA.

[*]These authors contributed equally to this work.
[5]Correspondence should be addressed to S.M.B. (e-mail: sblock@stanford.edu)

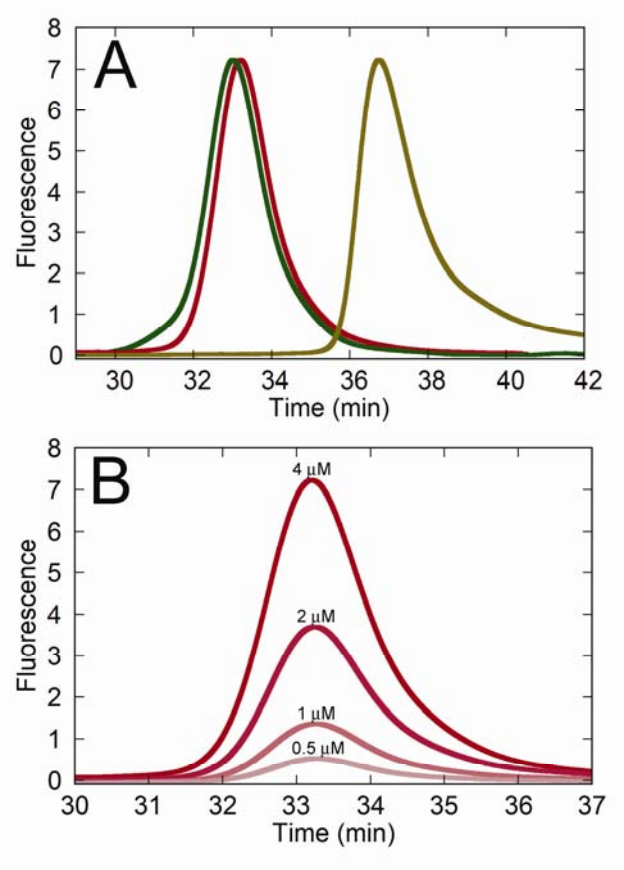

Figure S1 Analytical gel filtration profiles for Eg5 motors purified from *E. coli*. **(a)** Elution profiles monitoring intrinsic fluorescence *vs*. time for Eg5-513 (green), Eg5-513-5His (red), and Eg5-367 (brown). The void volume eluted at 16 min and the included volume at 51.5 min. The predicted value for M_r, based on the amino acid sequence for monomers is 57,644 Da for HsEg5-513, 58,787 Da for HsEg5-513-5His, and 41,667 Da for HsEg5-367. The oligomeric state was determined from plots of the partition coefficient, K_{av}, *vs.* log M_r (not shown). HsEg5-513: M_r = 189,688 Da; HsEg5-513-5His: M_r = 181,036 Da. **(b)** Gel filtration of HsEg5-513-5His at varying protein concentrations indicates that the dimeric state remains stable at low concentrations.

© 2006 **Nature Publishing Group**

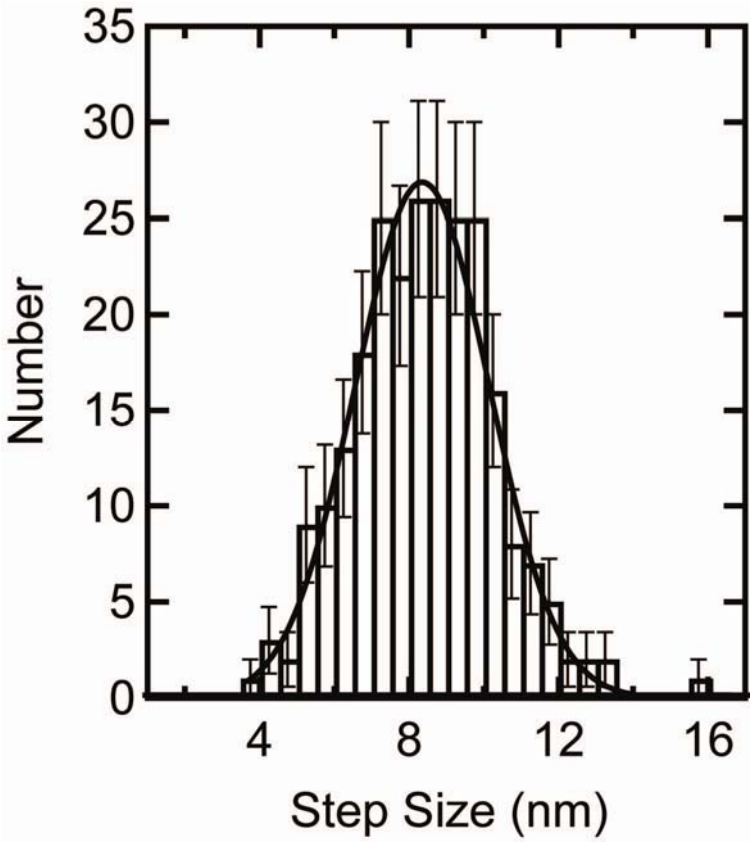

Figure S2 Histogram of step sizes for single Eg5-513-5His dimers (bin width, 1 nm; N = 257). A Gaussian fit to this distribution yielded a mean step size of 8.1 ± 0.1 nm, a distance consistent with the spacing of tubulin heterodimers along the microtubule protofilament. Note the absence of fractional or multiple step sizes, which can be generated when beads carry multiple motors.

© 2006 **Nature Publishing Group**

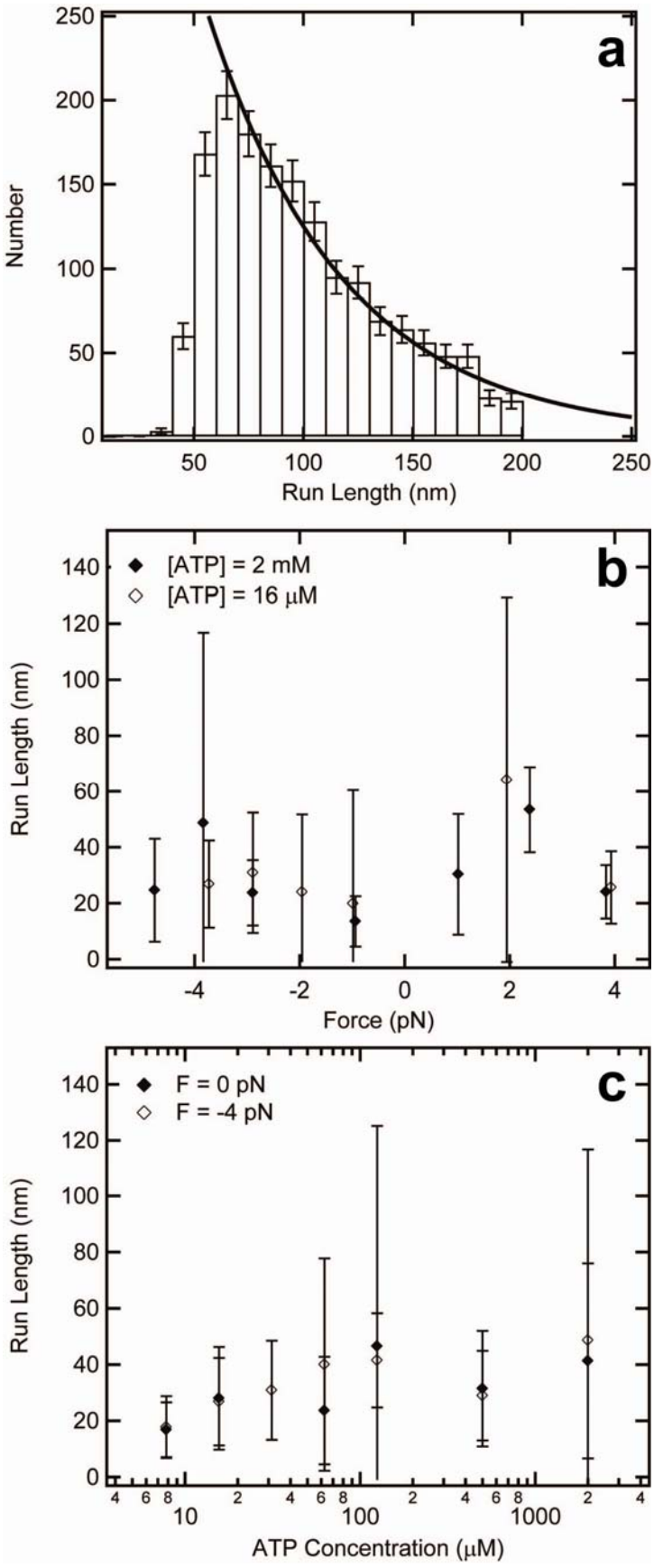

Figure S3 Run lengths are relatively insensitive to the applied load or to the ATP concentration. **(a)** Global histogram compiled from run lengths for all applied forces and ATP concentrations (N = 1,602; min. bin width 10 nm; all bins widths scaled to contain >6 counts). A small number of runs >200 nm exceeded the region reliably monitored by our instrument and were excluded. An exponential fit to this distribution (excluding the first three bins) yielded a mean run length of 63 ± 3 nm, in statistical agreement with the unloaded mean run length determined by video tracking (67 ± 7 nm)(*data in* ***Fig. 2h***). **(b)** Run length as a function of force at [ATP] = 2 mM (solid diamonds; n = 70−212 for each point) and [ATP] = 16 μM (open diamonds; n =57−80 for each point), determined by exponential fits to histograms of run length at each load. **(c)** Run length as a function of [ATP] at F = 0 (solid diamonds, n = 22−67 for each point) and F = −4 pN (open diamonds, n = 29−92 for each point), as determined by exponential fits to histograms of run length at each [ATP].

© 2006 **Nature Publishing Group**

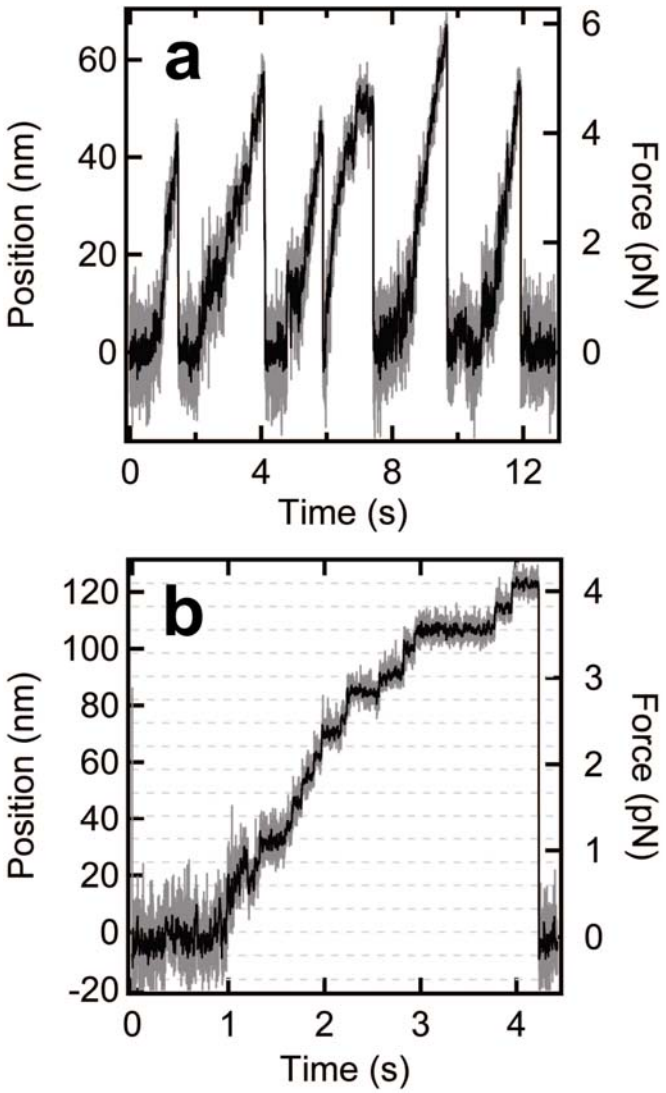

Figure S4. Stall force measurements with a fixed-position trap. Single Eg5 dimers step processively from the trap centre under monotonically increasing, hindering loads. **(a, b)** Representative records of bead motion. Median-filtered bead position (15-point window, black trace) is superimposed on the unfiltered position (grey trace). **(a)** Optical trap stiffness, k = 0.09 pN/nm. Beads moved out to ~65 nm from the centre of the trap, sustaining loads up to 6 pN. **(b)** Optical trap stiffness, k = 0.035 pN/nm. The bead moved 120 nm from the centre, sustaining a load up to 4 pN, before dissociating. Note that noise decreases at higher loads due to increased stiffness associated with the kinesin-bead linkage. As a consequence, 8-nm-sized steps are more apparent at higher loads.

© 2006 **Nature Publishing Group**

SUPPLEMENTARY INFORMATION

Dependence of K_M on load for Eg5 and conventional kinesin

For kinesin, k_b decreases more steeply than k_{cat} with load, causing K_M to increase[9]. For Eg5, however, k_{cat} and k_b appear to vary in equal proportion, making K_M independent of load. This disparity may be a consequence of differences in nucleotide affinity between the two motors For kinesin, the K_D for nucleotide binding is relatively high ($K_D = k_{-1}/k_1 \approx$ 400 μM) as compared with the unloaded K_M (~80 μM)[9]; therefore, the application of force can slow steps that occur after binding until K_M approaches K_D. In contrast, the unloaded K_M for Eg5 is just 14 μM, and fits to the three-state model (presented in the main text; see Fig. 3c) return a comparable value for K_D, leaving little 'headroom' for K_M to increase with force.

© 2006 Nature Publishing Group